

# **DIFFERENT MATHEMATICAL MODELLING APPROACHES TO PREDICT THE HORIZONTAL ANODE BAKING FURNACE PERFORMANCE**

Yasar Kocaefe<sup>1</sup>, Mounir Baiteche<sup>1</sup>, Noura Oumarou<sup>1</sup>, Duygu Kocaefe<sup>1</sup>,  
Brigitte Morais<sup>2</sup>

Yasar\_Kocaefe@uqac.ca<sup>1</sup>, Mounir.Baiteche1@uqac.ca<sup>1</sup>, Noura\_Oumarou@uqac.ca<sup>1</sup>,  
Duygu\_Kocaefe@uqac.ca<sup>1</sup>, Brigitte.Morais@alouette.qc.ca<sup>2</sup>

<sup>1</sup>University of Québec at Chicoutimi, Dept. of Applied Sciences, 555, boul. De l'Université,  
Chicoutimi, Québec, Canada G7H 2B1

<sup>2</sup>Aluminerie Alouette Inc., 400, Chemin de la Pointe-Noire, C.P. 1650,  
Sept-Îles, Québec, Canada, G4R 5M9

## **ABSTRACT**

The quality of carbon anodes has a considerable impact on the cell stability, energy consumption, environmental emissions, and the cost. The anode quality is influenced by many factors ranging from raw material properties to various process parameters. The anodes are baked in large furnaces and the final properties are fixed during this stage of production.

For the past number of years, mathematical modelling has become a powerful tool to study and analyze industrial processes. The field of anode baking was no exception. Various models have been developed and reported for the baking furnace analysis. Experimental studies of such complex systems are quite costly. The mathematical models provide an insight into the core of the operation. A process model and a 3D model (both dynamic) have been developed for horizontal anode baking furnaces, and they were validated using experimental data. All the important phenomena have been taken into consideration in the models.

The two models are being used to predict the performance of horizontal anode baking furnaces. In this article, the models will be described, the use of each model will be discussed, and the results of a number of practical applications for both models will be presented.

**Keywords:** horizontal anode baking furnace, mathematical modelling, carbon anodes, anode baking, process model, 3D model

## **INTRODUCTION**

The reduction of alumina by electrolysis in the Hall-Héroult process requires the use of carbon anodes for the primary aluminum production. Their quality (defined by their physical, electrical, chemical, mechanical, and thermal properties) has a strong influence on the process from cell stability and metal quality to energy consumption and environmental emissions. The raw material properties and all the process parameters have an impact on anode quality.

The prebaked anodes go through mainly three stages before their use in the electrolysis cell: green anode production in the paste tower, baking, and rodding. The granular material (coke, recycled butts and anodes) is mixed with a binder (pitch) to make a paste which is then fed to a vibrocompactor or a press to form green anodes. The green anodes are then cooled and stored until they are baked. Baking is the most costly step of the anode manufacturing process and also the last determining step for the anode quality.

The furnaces can generally be divided into two categories: horizontal and vertical. These furnaces consist of sections (usually 34 - 56) in two rows, and each one has two to three fire cycles at a time. This article is concerned with the modelling of the horizontal type anode baking furnaces. The sections consist of pits and flues. Packs of anodes are placed in the pit in multiple rows and columns depending on the size of the anodes and the pit dimensions, and then the rest of the space is filled with packing coke. Each pit is surrounded by refractory walls separating the anode and the packing coke from the gas required for the baking process. The enclosures that surround the pit on both sides and channel the gas are called flues. These furnaces behave like counter-current heat exchangers. The anodes are first heated and then cooled by the circulating gas. The packing coke supports the anode, provides a medium for heat transfer, and helps minimize the infiltration of air to the anode surface. The flue contains baffles and tie bricks to have a flow field that will provide, as much as possible, a uniform heat flow distribution for the baking of anodes.

Anodes are heated from room temperature to around 1100 °C at a prescribed heating rate and then cooled slowly. The entire cycle usually varies from two to three weeks. Each cycle covers 13-17 sections, part of which is shown in Figure 1. The ramps on the gas side are shifted after each fire cycle (approximately 20-30 hours). Anodes are not moved because moving them would require considerable handling and control issues to avoid their burning if exposed to air. Figure 1 shows a cycle with 3 preheating, 3 heating, and 6 cooling sections. The remaining sections of the cycle are used for the removal of baked anodes (the section after section 13), the preparation of anodes to be baked (the section preceding section 1), and repairs (the section before the one in which the anode are charged for baking).

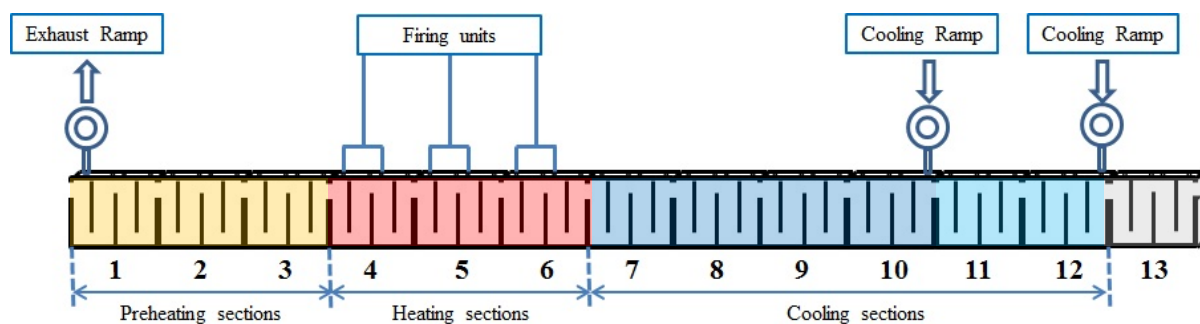


Figure 1: A schematic view of a fire cycle

Combustion of fuel (oil or natural gas), volatiles coming from the anodes (tar, methane, and hydrogen that are produced when the pitch is heated), and packing coke (which is undesirable, but unavoidable) provides the heating necessary for the entire system (anodes, refractories, and packing coke). Detailed information is given on the design and construction of these furnaces in reference [1].

Mathematical modeling has become a highly useful tool to study the impact of different operational and geometric parameters on furnace performance. This reduces the costly and long term plant trials. It should be noted that mathematical modeling is complementary to plant testing for any changes to furnace geometry or operation. It is difficult to carry out detailed measurements around the furnace due to cost and accessibility limitations. The models give an insight into the furnace behavior through the predicted distribution of temperature, flow, etc. Reference [2] gives a comprehensive review of the various modelling approaches.

Studies on the mathematical modelling of the anode baking furnaces were first seen at the beginning of the 1980's based on relatively simple approaches [3-5]. This is understandable given the availability of computing devices at the time. Then, rapid developments have taken place in numerical solution of differential equations and computing capacity (memory and speed). This led to the appearance of somewhat more sophisticated models [6-9]. A full 3D transient model was reported [10] in mid-1990s. Since then, many models of varying complexity have been published [11-15]; however, these are in general similar to the previously published models with some slight differences. Mathematical modelling is now a powerful tool in analyzing furnace operation and geometry.

## **MATHEMATICAL MODELLING**

Two different models were developed: a 3D model and a process model. The approach used in both models is similar. The gas and the solid parts of the furnace have completely different characteristics. Thus, the modelling work was divided into two parts: the flue which involves the calculation of pressures, velocities, and temperatures in a reacting gas flow (combustion), and the pit (including the refractory wall) which contains the anodes and the packing coke. The model takes into account the transient nature of the anode baking furnace operation. Two sub-models were developed for the two parts and were coupled through an interface which is located on the refractory wall surface on the flue side. The global model consists of these two coupled sub-models. Figure 2 shows the sub-models and the coupling. The modular approach makes the model development easier. Also, the sub-models could be used independently to study issues specific to flue or pit.

A large number of phenomena need to be considered in each sub-model. The flue sub-model has to account for the flow field (velocity and pressure distributions), combustion of fuel and volatiles, conductive, convective, and radiative heat transfer, air infiltration from various openings, volatiles coming from the anodes, and heat losses to environment. The pit model has to solve for the conduction heat transfer in all solids, devolatilization from the anodes (hydrogen, methane, and tar), coke combustion, air infiltration through packing coke, and heat losses to surroundings. The details of the geometry of both flue and pit have to be considered as well.

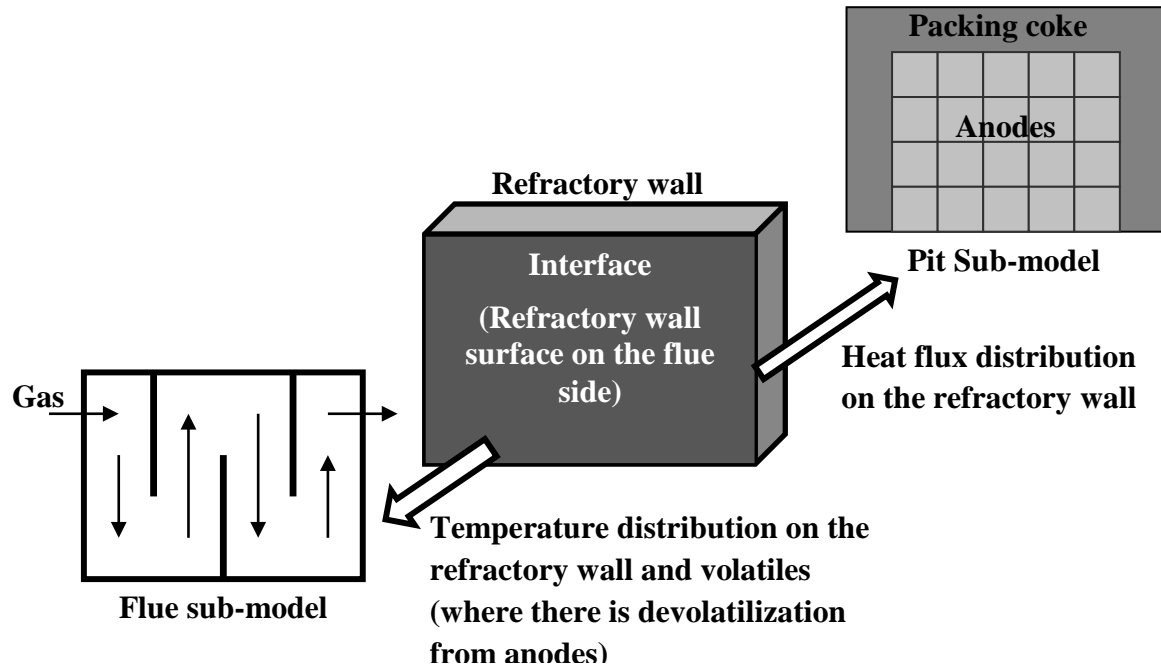


Figure 2: A schematic view of the flue and pit sub-models and their coupling

The progress in mathematical modelling has essentially followed the advancements in computing equipment design (memory and computational speed) and numerical methods for the solution of governing equations. Highly developed computing equipment and commercial numerical simulation codes are available today. Compared to the work done a few decades ago, such advancements allowed modelers to increase the mesh size many orders of magnitude and include more detailed of the physical phenomena described above.

Three-dimensional models can represent the geometry quite accurately and give comprehensive information on the distribution of all variables such as pressure, velocity, temperature, mass fractions, etc. However, this takes long computation time (many hours). Some of the issues could be resolved with less detailed models based on simpler approaches by eliminating such details as 3D velocity distribution or by neglecting gradients in certain directions and reducing the number of dimensions in the solution of equations. These are called process models. In these models, the computation time is much less (usually in minutes). Both models have their uses, and the best model is always the simplest one that provides the solutions needed to the issues of concern.

In the following sections, the 3D and process models are described. In both models, the temperature distribution on the brick wall (at the interface) calculated by the pit sub-model is used as the boundary condition for the flue sub-model, and the heat flux distribution calculated on the brick wall (at the interface) by the flue sub-model is used as the boundary condition for the pit sub-model (see Figure 2). In many cases, half of the pit and half of the flue were considered in both models based on the symmetry of the system. The entire geometry of the flue and/or pit was used when it was necessary. A number of measurement campaigns have been carried out to validate the models.

### 3D Model

In the flue, the following differential equations are solved:

- the continuity equation,
- the Navier-Stokes equation,
- the k- $\epsilon$  turbulence model equations,
- the heat transfer equation including all modes of transfer including radiation, and
- the transport equations for the chemical species (gas components) including combustion (of fuel and volatiles) [10, 12].

All are solved in 3D and under transient conditions, considering all the details of the geometry. The contribution by radiative heat transfer is calculated by the Monte Carlo method and is added to the energy equation which accounts for the radiative exchange between all components of the flue (gas and wall).

In the pit, the transient 3D conduction heat transfer equation is solved. The geometry is represented in detail. The volatile evolution from the anodes is calculated using the kinetic equations developed for this purpose [10]. The volatiles are then transferred to the flue for their combustion along with the fuel. The combustion of packing coke in the pit is treated empirically based on the coke temperature in zones exposed to air.

The air infiltration is calculated based on the pressure difference between the inside of the flue and the atmosphere in a way similar to orifice flow. Heat losses are determined using the overall heat transfer coefficients calculated at the domain boundaries.

The 3D model gives highly detailed information (3D velocity, temperature, and chemical species distributions, combustion and devolatilization patterns, etc.), but it takes a long time. Thus, it is not possible to simulate the entire cycle altogether, and only one section is simulated at a time. With this model, one section can be studied in great detail. The complete cycle also can be simulated by carrying out the calculation 'section by section' and each time using the outlet conditions from one section as the inlet conditions for the simulation of the following section. The partial differential equations are solved using the code ANSYS 15.0.

### Process Model

In the flue, the flow was simplified as shown in Figure 3. In the previous works reported in the literature, the flow was not considered at all, or it was taken as a 1D flow in the horizontal direction [5, 8, 15]. The actual flow is essentially vertical because of the baffles as can be seen in Figure 3. This simplification allows the calculation of the temperature distribution in the flue (gas and brick wall) in 2D (variation in the vertical and horizontal directions). This representation is more realistic for the flow in the flue. Thus, no relationship has to be adopted between the furnace length and the baking time, which was necessary for the process models in references [5, 8, 15] due to the consideration of flow only in the horizontal direction.

The pressure drop is calculated based on flow through a channel with a hydraulic radius. Each flue consists of four parts (the space between baffles), and each part is divided vertically into many cells. On each cell, overall mass, chemical species, and energy balances are carried out assuming pseudo steady-state condition. The transient process is accounted for by updating the above calculations at each time step.

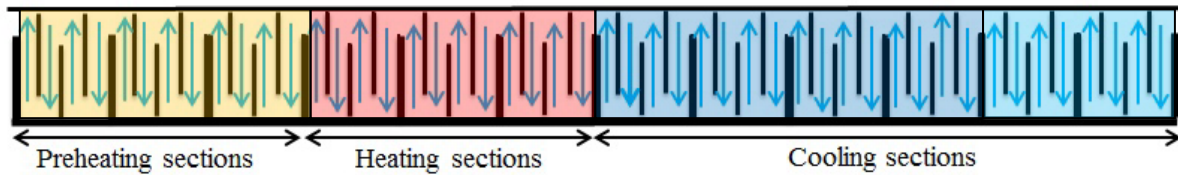


Figure 3: Representation of flow in the process model

In the pit sub-model, the 2D transient conduction heat transfer is solved using a fine mesh on vertical planes perpendicular to the refractory wall surface (in the transversal direction). There are four planes per section corresponding to the four parts in each section; however, this could be reduced to one plane per section (based on the average of four parts at any height in the flue). The devolatilization in the pit is calculated using the same kinetic equations as the ones in the 3D model. The volatiles coming from the anodes are transferred to the flue directly. The combustion patterns of volatiles and fuel are imposed.

The solution of the governing equations is programmed in FORTRAN, and the code was developed in our lab. At each time step, the calculations on the flue side are carried out for all sections using the brick wall temperatures as the boundary conditions. Then, the heat fluxes calculated by the flue side are used as the boundary conditions to solve the pit side equations on a large number of vertical planes one at a time.

The process model presented here is more detailed than the previous ones reported in the literature. More geometric details and more comprehensive representation of various physical phenomena can now be included in process modelling due to the availability of more powerful computing and numerical simulation tools today.

## RESULTS AND DISCUSSION

The results presented in this section except for the validation are obtained using a typical geometry which does not correspond to any industrial furnace.

### Process Model

The process model presented here involves many simplifications, but still gives relatively significant details to study the furnace performance. Figure 4 shows the calculation domains in the flue and the pit for one section. The calculations on the gas side (the flue sub-model) are carried out in the direction of flow (the imposed flow is shown by the blue arrows). The equations for the pit sub-model are solved on the four planes indicated by  $P_1$  to  $P_4$  in each section. Figures 5 and 6 show the calculated temperature profiles in the flue and in the pit, respectively, in section 2 of Figure 1 (second preheating section) at the end of one fire cycle. As can be seen in Figure 5, the temperatures vary in the horizontal and vertical directions, and the gas cools as it transfers heat to the refractory wall for the heating of anodes. The impact of the hot gases entering the flue is also clearly seen. In Figure 6, the 2D profiles on four planes give an indication of the temperature variation in the solids (refractory wall, coke, and anode) in the third direction (X). In this figure, two sets of figures for four planes are given. In the ones above, the horizontal scale is stretched to be able to give a better view of the temperature variation in the solids. However, the total width is actually much smaller than the height. The actual profiles (true scale) are given below. The left hand sides of the planes which are in contact with the gas (surface of the refractory wall) are hotter, and the temperature decreases towards the center (anodes). The process model calculates the temperature profiles in a similar manner in all sections.

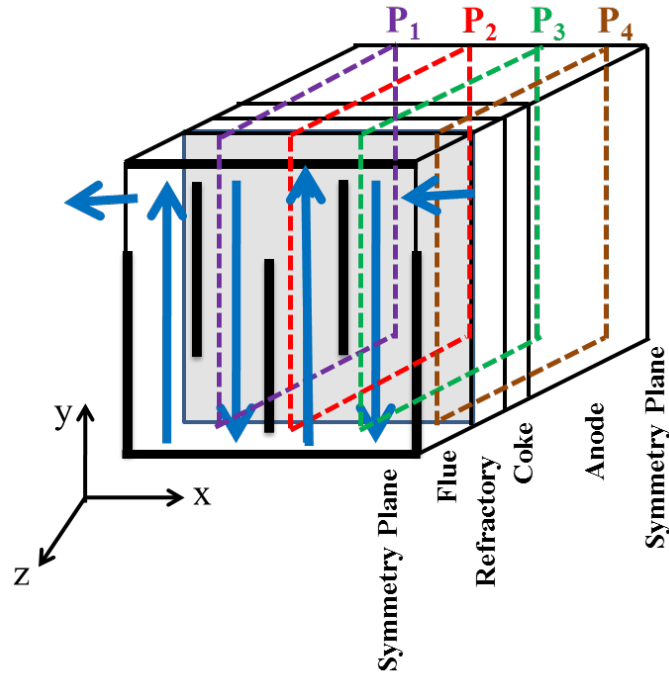


Figure 4: Flue and pit models (flow in the flue is shown with blue arrows; the four planes on which the pit equations are solved are illustrated as  $P_1$  to  $P_4$ ; interface is indicated by the light gray surface)

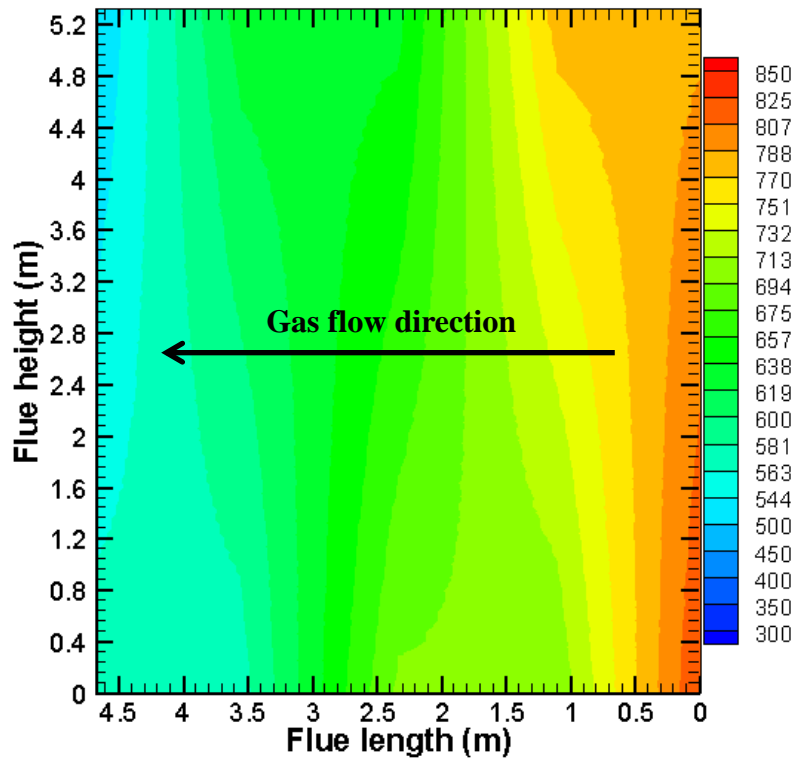


Figure 5: Gas temperature distribution predicted by the process model in the flue of the second preheat section of the furnace shown in Figure 1 (on XY plane in Figure 4) at the end of one fire cycle (the numbers for the scale indicate the temperature in  $^{\circ}\text{C}$ ).

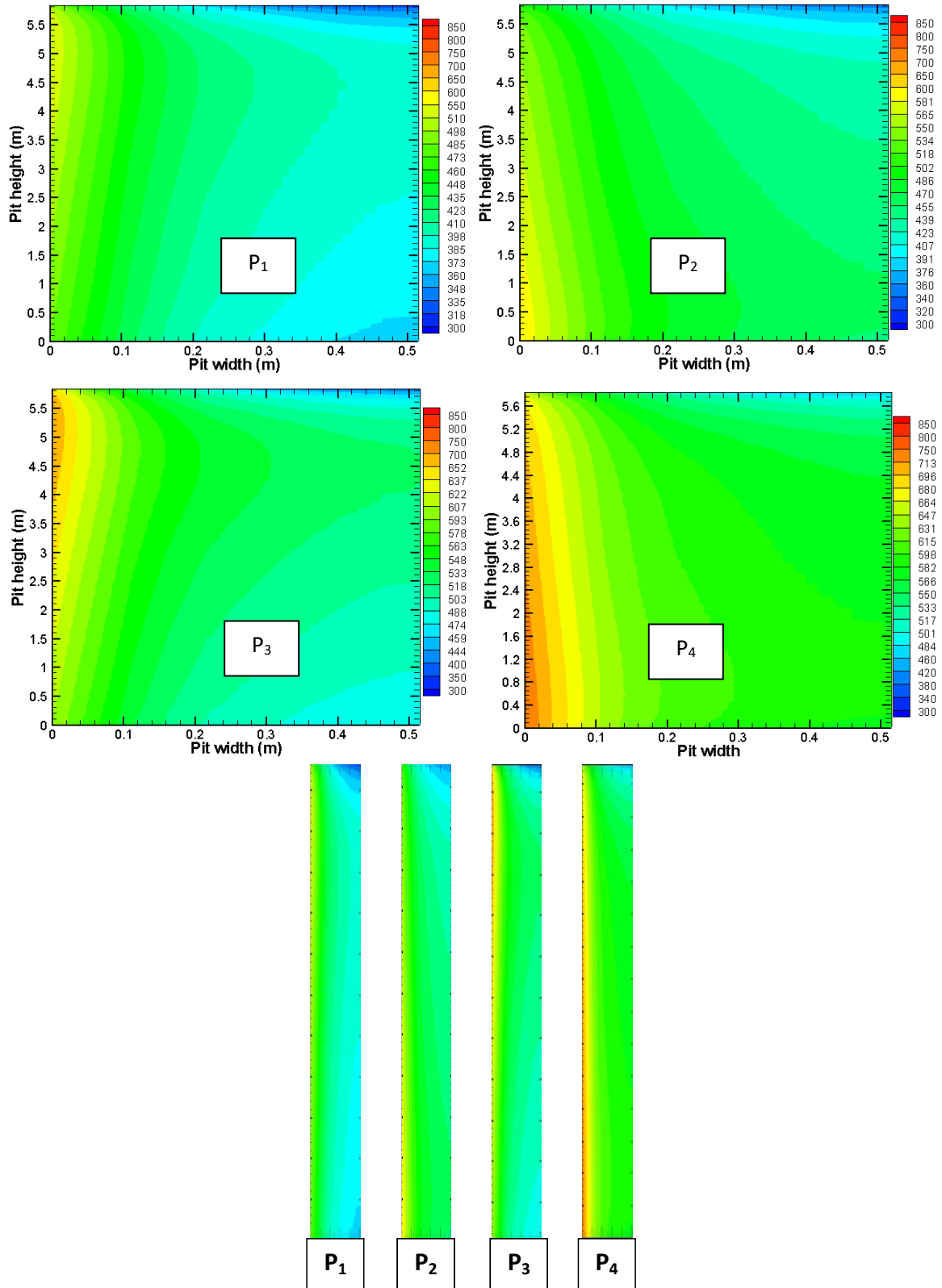


Figure 6: Temperature distribution predicted by the process model in the refractory wall and the pit (coke and anode) of the second preheat section of the furnace shown in Figure 1 on four planes (YZ planes in Figure 4) at the end of one fire cycle (the numbers on the scale indicate the temperatures in °C). The bottom figures are at actual scale. The width was stretched in the upper figures to give a more detailed view of the temperature distribution.



Figure 7 shows the average temperature profiles of the gas, the refractory wall, and the anodes along the furnace (a) after 7 hours of heating and (b) at the end of baking cycle (24 hours). After permutation (shifting all the ramps, taking out the section containing cooled anodes, and admitting a new section that contains green anodes into the cycle), the temperatures gradually increase till the end of the baking cycle. The volatiles that evolve from the anodes as they are heated are transferred to the flue for their combustion. The distribution of heat released due to volatile combustion depends on the choice of the user. In this case, the heat release was distributed uniformly across the flue, which resulted in the given temperature profile. In a large number of cases, a peak occurs in the third preheat section close to the first heating section due to a considerable quantity of volatile evolution and the transfer of these volatiles to the flue in this region of the furnace. It should also be noted that depending on the operation, such a peak may not occur.

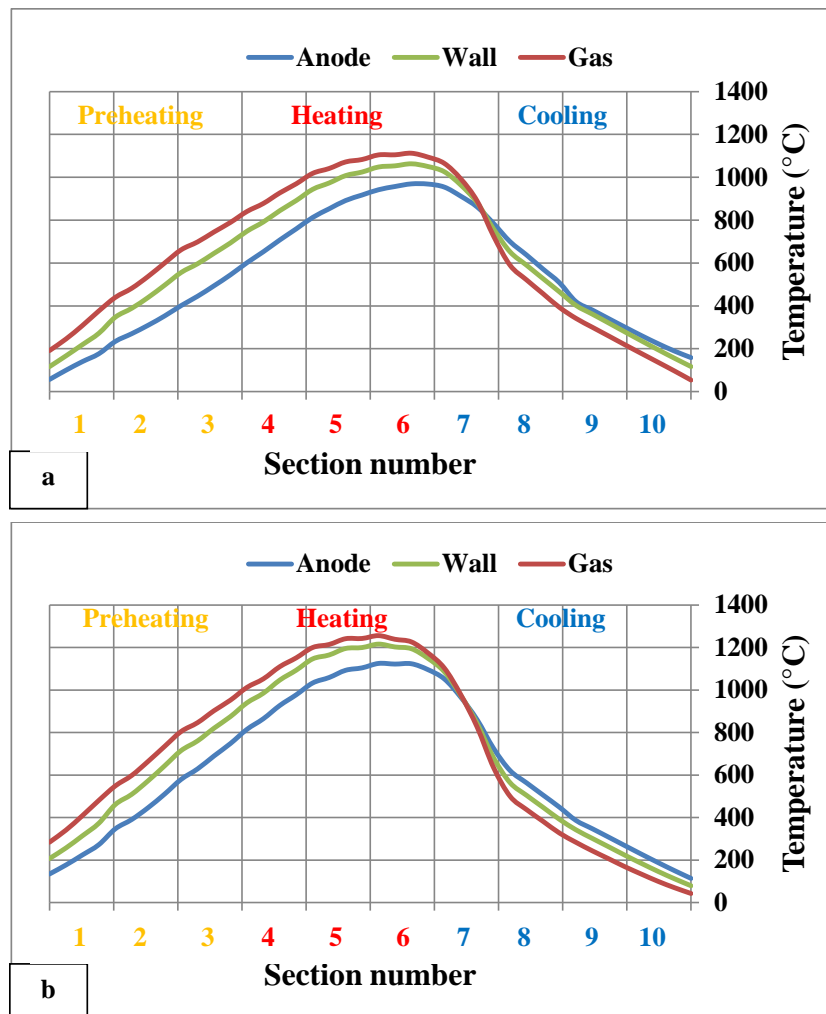


Figure 7: The average gas, refractory wall, and anode temperatures along the furnace: (a) after 7 hours of heating and (b) at the end of cycle (for section numbers, see Figure 1).

Figure 8 gives (a) the mass fraction of oxygen, (b) the variation of pressure (difference between the pressure in the flue and the atmospheric pressure), and (c) the profiles of combustion products along the furnace. The mass fraction of oxygen remains constant in the cooling sections and then starts to decrease as it is consumed due to the combustion of fuel and volatiles. This is accompanied by the generation of combustion products, namely water vapor and carbon dioxide, as the combustion proceeds from heating to preheating sections. The pressure decreases along the furnace as expected. On the left hand side of the zero-

pressure position (where the pressure in the flue is equal to the atmospheric pressure), the pressure values become negative (less than atmospheric). Here the mass flow rate increases due to air infiltration resulting in a slightly non-linear profile for the pressure. Air infiltration and the pressure values are intimately related. In this case, the total air infiltration was 10% of the total flow in the cooling section. When the amount of air infiltration increases, the curvature of the line becomes more pronounced. The amount of infiltration depends on the size of openings set in the model. This can be varied to simulate different infiltration rates.

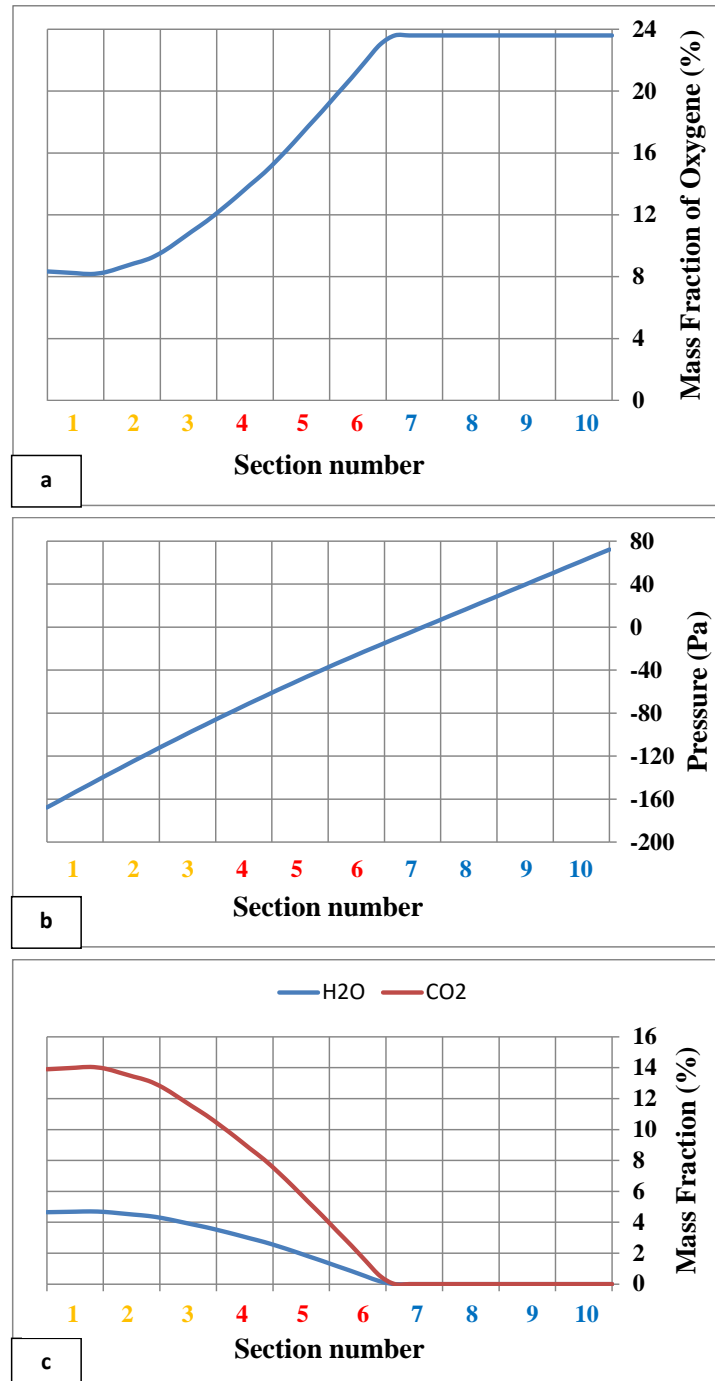


Figure 8: (a) Mass fraction of oxygen, (b) pressure drop, and (c) mass fractions of combustion products (water vapour and carbon dioxide) along the furnace.

The process model gives relatively comprehensive information on furnace behaviour, which could be used to test furnace performance under different operating conditions. Optimization could be done by carrying out parametric studies.

### 3D Model

Experimental data obtained through measurement campaigns have been used to validate the models partially or totally depending on the data set. Figure 9 shows normalized maximum temperatures predicted (by the 3D model) and measured at a number of positions on the top of the anodes in the top row in a pit. Two types of measurements were taken. The thermocouples were placed in contact with the anode surface where the predicted temperatures are also shown. The second measurement was carried out using green coke placed in crucibles and then measuring the crystalline lengths ( $L_c$ ) of the samples. The  $L_c$  values are correlated with temperatures which show the maximum value reached at that position. The crucibles were placed in the packing coke above the anodes and thus their lower values are justified. The method used for the calculation of radiative heat transfer in the flue is important, and the results presented in Figure 9 were obtained with the Monte Carlo method which is one of the most accurate methods. In Figure 9, there is a good agreement in general between the predicted and measured values except at the first position very close to the side of the pit. The gas composition is important for the radiative heat transfer calculations. The discrepancy is quite likely due to the inexactness of the gas composition here which affects heat transferred to the refractory surface and consequently the entire heat transfer in the pit. The work is still continuing on model validation.

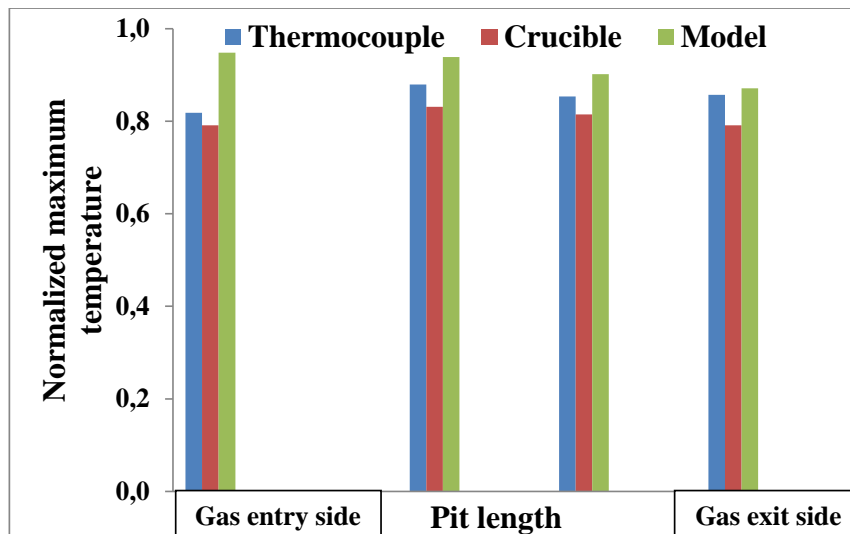


Figure 9: Calculated (Model) and measured temperatures (Thermocouple and Crucible) on the top surface of the anodes in the top row in a furnace.

In Figures 10 and 11, all the temperatures (flue, refractory wall, packing coke, and anodes; flue on the left and anodes on the right) are shown at different stages of the baking process from (a) to (f). In Figure 10, all figures are given over a range of 1300 °C to be able to view the temperature profiles over the overall range. In Figure 11, the temperature scales are arranged according to the range of data in each figure to visualize the profiles better. The impact of the direction of gas flow is also evident on all profiles. In earlier works published in the literature [10, 12, 14], the baffles and the tie bricks in the flue were not usually taken into account in the heat transfer calculations. With the new codes, it is possible to consider all geometrical factors in the simulation. The impact of the presence of the baffles and tie bricks

on the temperature profiles can be seen. This impact seems to nearly fade away in the anode region.

The flue walls (refractories) deform after a certain number of fire cycles. This was studied by taking a flue and deforming both of its walls in the same direction by 30 mm in the center as shown in Figure 12. The deformation could occur differently in different furnaces and could result in various forms for the walls. All forms could be studied using the 3D model. Figure 13 shows the flow fields on four planes in a normal flue and in a deformed flue. The change in the flow field is clearly seen. Due to deformation, the velocities on one side are higher than the other side. This will create differences in the baking of the anodes in two adjacent pits which will have an impact on the quality of the anodes produced.

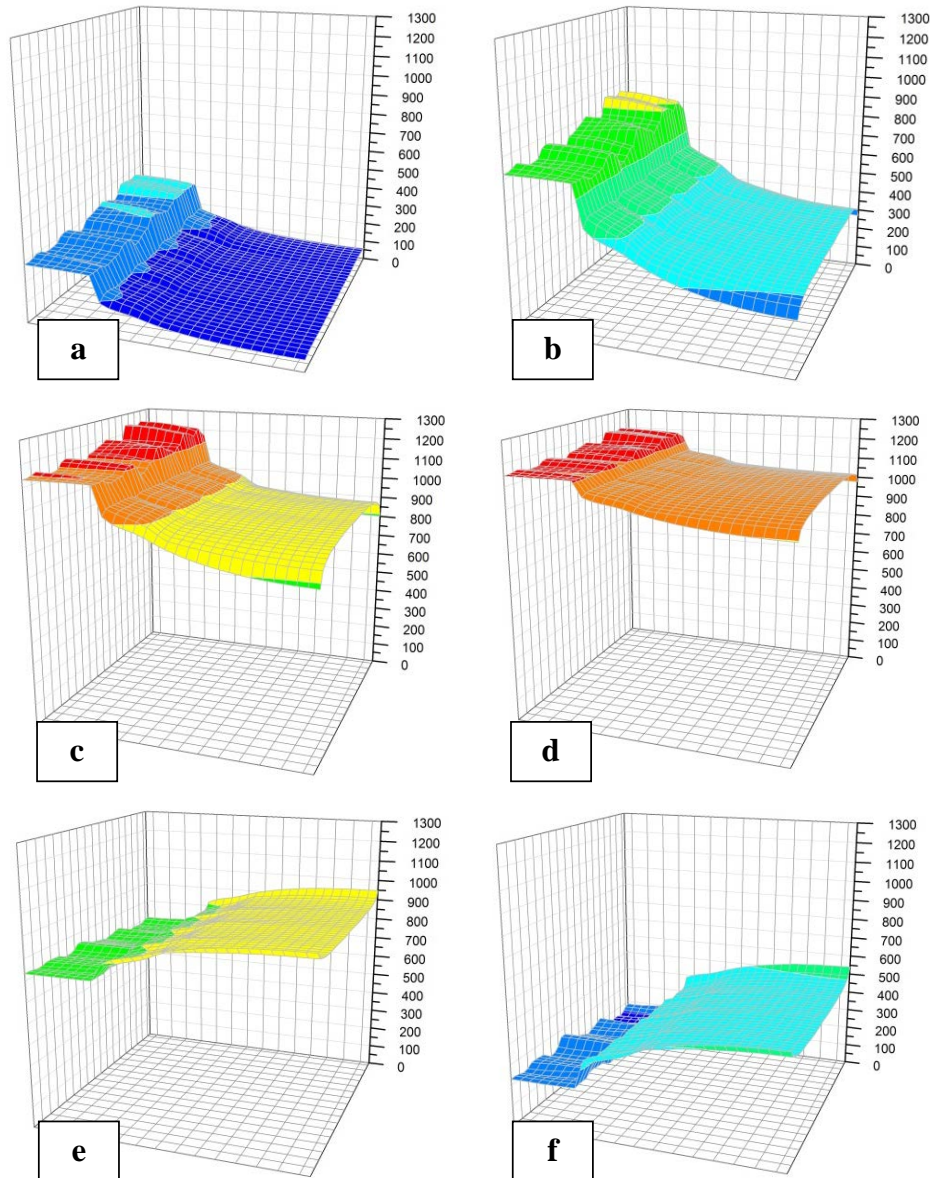


Figure 10: Temperature profiles in the pit, refractory wall, and flue at different stages of the baking process (the numbers indicate the temperatures in °C; the temperature scales are over 1300 °C to be able to view the results based on the overall range): (a) preheating (section 1), (b) preheating (section 2), (c) heating (section 4) (d) soaking (section 6), (e) cooling (section 7), and (f) cooling (section 8).



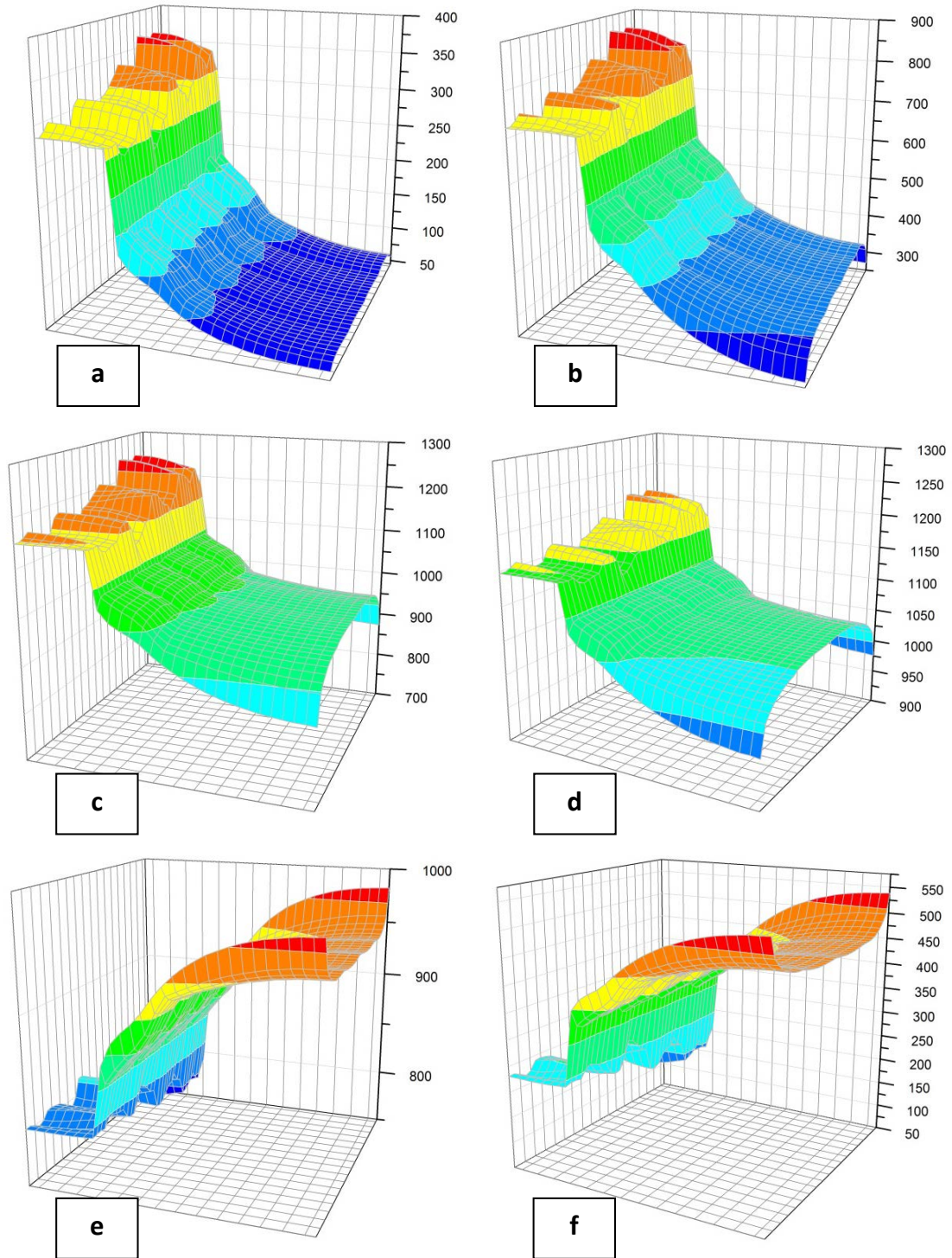


Figure 11: Temperature profiles in the pit, refractory wall, and flue at different stages of the baking process (the numbers indicate the temperatures in  $^{\circ}\text{C}$ ; the temperature scales are arranged according to the range of data in each figure to visualize the profiles better): (a) preheating (section 1), (b) preheating (section 2), (c) heating (section 4) (d) soaking (section 6), (e) cooling (section 7), and (f) cooling (section 8).

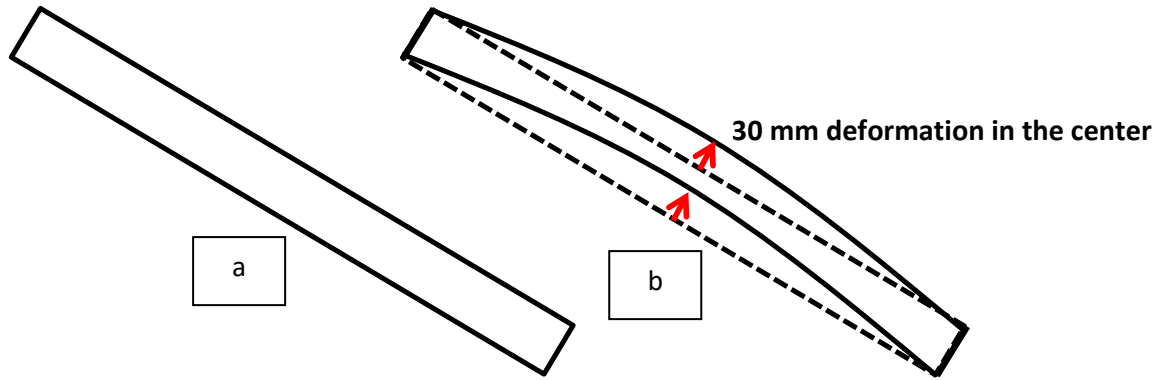


Figure 12: Schematic representation of the deformation from the top view of the flue (a) normal flue and (b) deformed flue

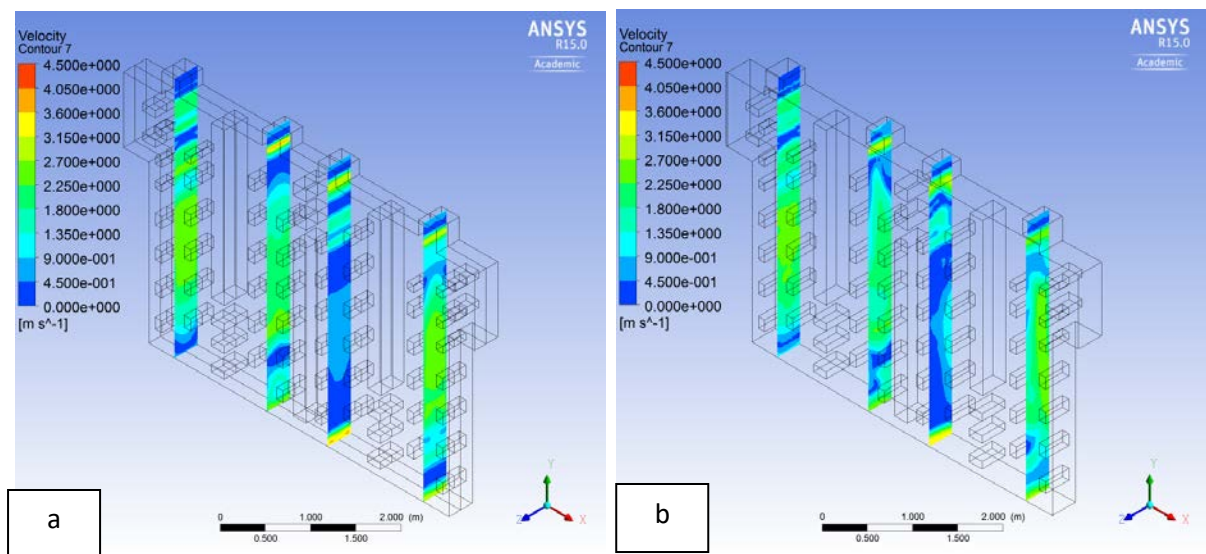


Figure 13: Comparison of (a) the flow field in a normal flue with (b) the one in a deformed form of the same flue (geometry from [16]).

## CONCLUSIONS

An overall view on the mathematical modelling of the horizontal anode baking furnaces is presented. The two models developed (3D and process) are described. The capabilities of each model are discussed. The 3D model requires long computation times, but gives detailed information on the furnace behavior. This model is needed for major changes in geometry and operation. The process model is better suited for the study of changes in operation and control, gives fewer details, but requires much less computation time. Some of the results obtained with the two models are presented and discussed.

## ACKNOWLEDGEMENTS

The technical and financial support of Aluminerie Alouette Inc. as well as the financial support of the National Science and Engineering Research Council of Canada (NSERC), Développement économique Sept-Îles, the University of Québec at Chicoutimi (UQAC), and the Foundation of the University of Québec at Chicoutimi (FUQAC) are greatly appreciated.

## REFERENCES

1. F. Keller & P.O. Sulger, Anode Baking (R&D Carbon, 2<sup>nd</sup> Edition Sierre, Switzerland, 2008.
2. A Charette, Y Kocaefe & D Kocaefe, Le carbone dans l'industrie d'aluminium (La Presses de l'aluminium, PRAL, Chicoutimi, Quebec, Canada, 2012)
3. A Furman & H Martirena, A Mathematical Model Simulating an Anode Baking Furnace, Light Metals (AIME), 1980, 545-552.
4. M A Thibault, M.A., R T Bui, A Charette & E Darnedde, Simulating the dynamics of the anode baking furnace, Light Metal, 1985, 1141-1151.
5. R T Bui, A Charette & T Bourgeois, Performance analysis of the ring furnace used for baking industrial carbon electrodes, The Canadian Journal of Chemical Engineering, 1987, 65, 96-101
6. T Bourgeois, R T Bui, A Charette, B A Sadler & A D Thomsett, Computer Simulation of a vertical ring furnace, Light Metals, 1990, 547-552.
7. M Jacobsen & M C Melaaen, Heat and Mass Transfer in Anode Materials During Baking, Light Metals, 1995, 681-690.
8. R Ouellet, Q Jiao, E Chin, C Celik, D Lancaster & D Wilburn, Anode baking furnace modeling for process optimization, Light Metals, 1995, 653-662.
9. R T Bui, S Peter, A Charette, A D Tomsett & V Potocnik, Modelling of heat transfer and gas flow in the vertical flue anode baking furnace, Light Metals, 1995, 663-671.
10. Y Kocaefe, E Darnedde, D Kocaefe, R Ouellet, Q Jiaon & W F Crowell, A 3D mathematical model for the horizontal anode baking furnaces, Light Metals, 1996, 529-534.
11. L Zhang, C Zheng & M Xu, Simulating the heat transfer process of horizontal anode baking furnace, Dev. Chem. Eng. Mineral Process., 2004, 12(3/4), 427-440.
12. D S Severo, V Gusberti & E C V Pinto, Advanced 3D modelling for anode baking furnaces, Light Metals, 2005, 697-702.
13. F Keller, U Mannweiler, & D S Severo, Computational Modeling in Anode Baking, R&D Carbon Ltd., Sierre, Switzerland, August 2006, 1-12.
14. D S Severo, V Gusberti, P Sulger, F Keller & M W Meier, Recent developments in anode baking furnace design, Light Metals, 2011, 853-858.
15. D S Severo & V Gusberti, User-friendly Software for Simulation of Anode Baking Furnaces, 10<sup>th</sup> Australasian Aluminum Smelting Technology Conference, 2011, 18 pages.
16. E S Chen, Thermomechanical improvement of a flue wall in anode baking furnace, Unitecr'95, vol. 3, 1995, pp. 432-433.